ICES Journal of Marine Science, 2023, **0**, 1–12
DOI: 10.1093/icesjms/fsad007
Original Article

Asymmetry in the rate of warming and the phenology of seasonal blooms in the Northeast US Shelf Ecosystem

Kevin D. Friedland [1,*], Nicholas R. Record [2], Daniel E. Pendleton [3], William M. Balch [2], Karen Stamieszkin [2], John R. Moisan [4] and Damian C. Brady [5]

[1]National Marine Fisheries Service, Narragansett, RI 02882, USA
[2]Bigelow Laboratory for Ocean Sciences, East Boothbay, ME 04544, USA
[3]Anderson Cabot Center for Ocean Life, New England Aquarium, Boston, MA 02110, USA
[4]Wallops Flight Facility, Goddard Space Flight Center, Wallops Island, VA 23337, USA
[5]School of Marine Sciences, University of Maine, Walpole, ME 04573, USA

[*] *Corresponding author:tel: +401 782-3236;* e-mail: kevin.friedland@noaa.gov.

Predicting the impact of marine ecosystem warming on the timing and magnitude of phytoplankton production is challenging. For example, warming can advance the progression of stratification thereby changing the availability of nutrients to surface phytoplankton, or influence the surface mixed layer depth, thus affecting light availability. Here, we use a time series of sea surface temperature (SST) and chlorophyll remote sensing products to characterize the response of the phytoplankton community to increased temperature in the Northeast US Shelf Ecosystem. The rate of change in SST was higher in the summer than in winter in all ecoregions resulting in little change in the timing and magnitude of the spring thermal transition compared to a significant change in the autumn transition. Along with little phenological shift in spring thermal conditions, there was also no evidence of a change in spring bloom timing and duration. However, we observed a change in autumn bloom timing in the Georges Bank ecoregion, where bloom initiation has shifted from late September to late October between 1998 and 2020—on average 33 d later. Bloom duration in this ecoregion also shortened from ∼7.5 to 5 weeks. The shortened autumn bloom may be caused by later overturn in stratification known to initiate autumn blooms in the region, whereas the timing of light limitation at the end of the bloom remains unchanged. These changes in bloom timing and duration appear to be related to the change in autumn thermal conditions and the significant shift in autumn thermal transition. These results suggest that the spring bloom phenology in this temperate continental shelf ecosystem may be more resilient to thermal climate change effects than blooms occurring in other times of the year.

Keywords: climate change, continental shelf, phenology, phytoplankton blooms, temperature.

Introduction

There is a concern that climate change may alter the dynamics of phytoplankton blooms in marine ecosystems, thus causing phenological mismatches within oceanic food webs (Henson *et al.*, 2018). Many taxa, including important resource species, time their reproductive cycles to best utilize the productivity of the vernal seasonal bloom, a relationship that is expected to erode over time (Asch *et al.*, 2019). Blooms that occur earlier than climatological norms may benefit some species (Kristiansen *et al.*, 2011); however, a delay in the spring bloom can provide improved feeding conditions for resource species, such as the larval life stage of the Japanese sardine (Kodama *et al.*, 2018). A bloom cycle composed of a single vernal bloom cannot be generalized to all marine ecosystems; some systems, like the subject system of this study, have an annual bloom cycle that also includes an autumnal bloom. The autumnal seasonal bloom plays a role in resource species reproduction by providing provisioning nutrition to pre-spawning adults (Leaf and Friedland, 2014). Hence, the phenology of all seasonal blooms that are characteristic of an ecosystem have the potential to affect species reproduction.

It is also important to consider the disruption that altered bloom phenology can have on energy transfer among trophic groups. In the Baltic Sea, early spring blooms were attributed to taxa-specific responses of diatoms and dinoflagellates to changing climate conditions, which in turn played an important role in altering the transfer of energy to the benthos (Hjerne *et al.*, 2019). Bloom timing is expected to have a mixed response to climate change in the sense that forcing factors, which vary by latitude, may cause some regions to experience advances in bloom timing, while others may see delays (Henson *et al.*, 2018). The syncopation of food webs in both aquatic and terrestrial ecosystems will likely have societal impacts, not least of which includes the erosion of food security provided by marine fisheries (Stevenson *et al.*, 2015).

The Northeast US Continental Shelf (NES) marine ecosystem has already experienced rapid and substantial warming; however, there is evidence that warming may be seasonally asymmetric. The change in NES temperature has been variously estimated (Kavanaugh *et al.*, 2017), but what is clear is that change in temperature has intensified in recent years (Friedland *et al.*, 2020a). Prominent in the time course of thermal change in the NES has been a change point in both surface and bottom water temperature, that may be a leading indicator of a regime shift in conditions defining the oceanography of the system (Record *et al.*, 2019a; Gonçalves Neto *et al.*, 2021). In fact, the NES is among the fastest-warming marine ecosystems worldwide (Pershing *et al.*, 2015, 2021). However, this increase in temperature has not been uniform across the annual cycle (Thomas *et al.*, 2017), featuring an increase in annual SST range caused by rapid warming in

Received: April 29, 2022. **Revised:** December 21, 2022. **Accepted:** January 4, 2023

summer and the maintenance of winter temperatures (Friedland and Hare, 2007). There also has been an intensification of the hydrological cycle, particularly in the Gulf of Maine (Balch *et al.*, 2012), with more anomalous drought and flood years, which were associated with step changes in physical, biological, chemical, and optical properties. While seasonally colder winter temperatures have been noted for much of the Northern Hemisphere (Cohen *et al.*, 2012), asymmetry in warming and cooling can manifest itself in different latitudinal gradients of warming (Xu and Ramanathan, 2012) and is also the case where cooling extremes seem to be intensifying compared to warming extremes (Li *et al.*, 2021).

The NES ecosystem is part of the western boundary of the Atlantic basin and is characterized by complex bathymetry with shelf areas of varying width, deep basins, and an elevated bank (Sherman *et al.*, 1996). The physical structure of the ecosystem contributes to the phenology of phytoplankton bloom patterns that are continuous with trans-Atlantic patterns of either bimodal or a single autumn/winter annual bloom cycle (Friedland *et al.*, 2016). The northern part of the ecosystem tends to have spring and autumn blooms, with maximum chlorophyll concentrations temporally uncorrelated with maximum of primary productivity. The spring bloom in the northern NES is driven by nutrient inputs from deep, off-shelf waters that enter the ecosystem via the Northeast Channel in the Gulf of Maine (Townsend *et al.*, 2010), and which reflect variation in the source waters contributing to this flow (Townsend *et al.*, 2006). The relative proportions of Labrador Current and shelf slope source waters set the nutrient content and salinity in the region (Townsend *et al.*, 2010). During later winter, wind driven mixing replenishes nutrients in surface waters, which along with increasing day length and solar elevation, form the ideal conditions for a spring bloom. Historical data recovery suggests that both spring and autumn blooms in the Gulf of Maine have long-term trends of delayed bloom start date on a century scale (Record *et al.*, 2019b). However, contemporary bloom timing may be associated with other factors such as salinity, which in turn can be related to the changing pattern of Arctic inflow into the Gulf of Maine (Song *et al.*, 2010). Despite a high degree of variability, there does not appear to be a directional trend in spring bloom timing or magnitude in recent decades (Friedland *et al.*, 2015a). The occurrence of autumn bloom tends to be more variable (Friedland *et al.*, 2015b) and its initiation has been linked to water column stability (Song *et al.*, 2011). Though blooms in the northern part of the NES tend to be dominated by diatoms and dinoflagellates, *Synechococcus* spp. blooms are also often prominent in coastal areas and appear to be controlled by temperature (Hunter-Cevera *et al.*, 2016).

The annual production cycle of the southern NES is very different from the north. The pattern of seasonal blooms appears to be replaced by an extended period of elevated surface chlorophyll concentration starting in autumn and extending into winter. As in the north, primary productivity does not necessarily correlate with chlorophyll concentration. However, unlike the north, waters on the Mid-Atlantic shelf are often mesotrophic and rainfall in the region plays an important role providing nutrients via runoff (Sedwick *et al.*, 2018). The nutrients associated with runoff also contribute to new production in the region. Though river discharge is important in the southern NES, physical forcing such as wind mixing also plays an important role (Xu *et al.*, 2020). The Mid-Atlantic Bight "cold pool" provides a cold refuge for many species (Chen *et al.*, 2018), but the strong water column stratification necessary to maintain it acts as a barrier to water column mixing and nutrient replenishment; therefore, much of the primary productivity of the Mid-Atlantic Bight is not new production, but rather regenerated production supported by microbial nutrient recycling.

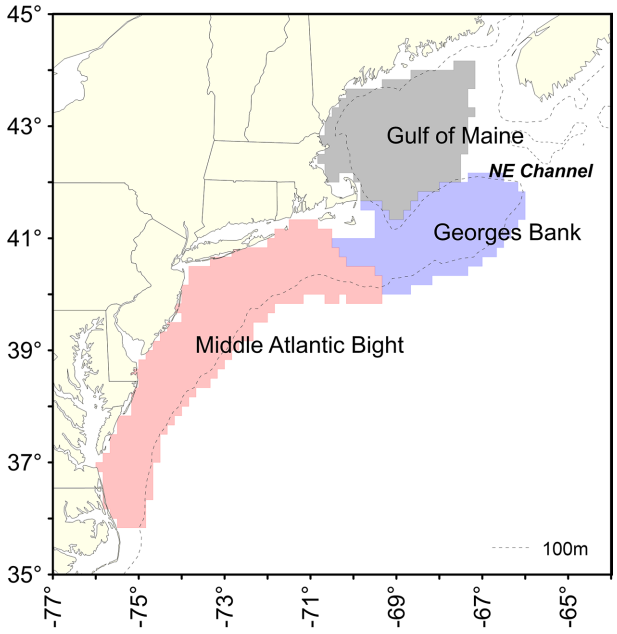

Figure 1. Map of the US Northeast Shelf Ecosystem with the GBK, GOM, and MAB ecoregions indicated.

The goals of this study were twofold. First, to examine more closely the seasonal asymmetry in ecosystem warming occurring in the NES. The second goal was to test whether any change in thermal conditions may be related to change in seasonal phytoplankton bloom dynamics. To achieve the first goal, we examined high-resolution temporal data on sea surface temperature to test where, and when during the year, changes had occurred within ecological subareas or ecoregions of the NES. The change in thermal environment was also characterized with seasonal phenology indices. The second goal was achieved by estimating bloom-timing metrics, spatially aligned to the same ecoregions. We present findings of significant change to some aspects of thermal and bloom phenology on the NES, as well as signs for notable resilience to change.

Methods

Study system

The thermal and phytoplankton bloom phenology of the US Northeast Continental Shelf Ecosystem was analysed over three ecoregions (Figure 1), the Georges Bank (GBK), Gulf of Maine (GOM), and Middle Atlantic Bight (MAB). Ecoregion partitioning is based on a multivariate analysis of physical and biological parameters and is commonly used in various ecosystem assessments. Sea surface temperature and chlorophyll concentration remote sensing products were extracted from global databases based on the geographic shapes of the ecoregions.

Seasonal trends in SST

Thermal trend and phenology were based on sea surface temperature extracted from the Optimum Interpolation Sea Surface Temperature (OISST) database version 2.1 for the period 1997–2020 (see data availability statement). The dataset, which has a spatial resolution of 1/4° and daily temporal resolution, is constructed by combining observations from different platforms (satellites, ships, buoys, and Argo floats) on a regular global grid (Reynolds *et al.*, 2007). Mean temperatures and trends were evaluated by ecoregion and day of the year. In addition to the analysis of the trend in SST data, thermal phenology was also characterized by determining spring and autumn transition days of the year (Friedland *et al.*, 2015a). For each ecoregion, the time series average SST was determined. The SST data for a given year were smoothed with a 5-point moving average filter and the first day of the year that exceeded the transition temperature, taken as the average SST, was considered the spring transition date and the first day the SST fell below that temperature was considered the autumn transition date. The trend in the SST and transition dates was estimated using the generalized least squares model selection approach described in Hardison *et al.* (2019). This approach fits trend models with Gaussian, AR(1), and AR(2) correlation structures prior to selection by small-sample AIC, and reduces estimation bias due to autocorrelated residuals when compared to linear regression or the Mann–Kendall test alone.

Phytoplankton bloom phenology

Phytoplankton bloom phenology was based on bloom parameters derived from time series of chlorophyll concentration (CHL) and using a change point algorithm of bloom detection. CHL data was retrieved from the Hermes GlobColour website (see data availability statement) at a spatial resolution of 4 km and temporal resolution of 8 d over the period 1998–2020. The CHL data were a merged product using the Garver, Siegel, Maritorena Model (GSM) that combined the data using a bio-optical model inversion algorithm (Maritorena *et al.*, 2010). The procedure combines data from Sea-viewing Wide Field of View Sensor (SeaWiFS), Moderate Resolution Imaging Spectroradiometer on the Aqua satellite (MODIS), Medium Resolution Imaging Spectrometer (MERIS), Visible and Infrared Imaging/Radiometer Suite (VIIRS), and Ocean and Land Colour Instrument (OLCI) sensors. These passive satellite remote sensing data provide a weighted average of the chlorophyll concentration in the top two optical depths of the sea, typically 5–15 m depth depending on water clarity (Gordon and McCluney, 1975). The performance of this CHL data product was compared to the OC5 CHL product disseminated via CMENS (data.marine.copernicus.eu), which is a product sensitive to case water types. The comparison was based on *in-situ* CHL from the Would Ocean Database and restricted to observations within the NES proper. The OC5 data performed better within ∼15 km of the coastline based on correlation analyses. However, over much of the NES, the GlobColour CHL produced slightly higher correlations with the *in-situ* data; hence, we elected to use the GlobColour in our study.

Bloom phenology parameters, bloom start day of the year and duration, were calculated using the same change point algorithm used in both regional and global analyses of bloom dynamics. Bloom periods were identified with the change point algorithm sequential *t*-test analysis of regime shifts (STARS) (Rodionov, 2006). A bloom was detected when a change point from low to high CHL was detected with the added condition that a change from high to low CHL also could be found to demarcate the bloom period. The STARS algorithm was parameterized following an extension of the method intended to increase bloom detection sensitivity (Friedland, 2021). The STARS α parameter was tested at the values of 0.05, 0.1, and 0.15; length criteria at values of 4, 5, and 6; and Huber weight at values of 2, 3, and 4. In previous assessments, blooms that exceeded a duration of nine 8-d periods were considered ecologically different from discrete blooms and were excluded from the analysis (Friedland *et al.*, 2015b). For each bloom detection, a bloom start day of the year was determined along with a bloom duration expressed as the number of 8-d periods associated with the event. The same approach for the estimation of trend used in the temperature data was used with the bloom data. Finally, the bloom analysis was used to estimate mean bloom periods for each ecoregion that were used graphically in the figures showing mean daily SST and trend.

Results

Change in thermal phenology

The timing of seasonal thermal transitions is generally similar across the three ecoregions with higher temperatures and slightly earlier transitions in the MAB compared with the GBK and the GOM. The thermal cycle for the GBK ecoregion SST has a winter minimum of ∼5.3°C and a summer maxima of 19.1°C (Figure 2a). The winter minima generally occurred in early March and the summer maxima occurred in late August; both these periods are also associated with higher level of interannual variability. The change in SST by day of the year for the GBK ecoregion is sinusoidal with a winter minimum 0.20°C decade^{-1} and a summer maximum of 0.82°C decade^{-1} (Figure 2b). The same patterns exist in the GOM and MAB ecoregions. The GOM SST extremes are bracketed at 4.5 and 18.1°C (Figure 2c) and change in SST ranges from 0.46 to 1.15°C decade^{-1} (Figure 2d) and the MAB SST extremes are bracketed at 6.6 and 24.2°C (Figure 2e) and change in SST at 0.13 and 0.69°C decade^{-1} (Figure 2f). The dates of winter minima and summer maxima in the GOM were similar to GBK; however, these extremes tended to occur earlier (by a week or so) in the MAB. For all ecoregions, the significant daily slopes were mainly in the summer portion of the year, whereas non-significant slopes were concentrated in the winter portion (Figure 2b, d, and f).

Seasonal differences in temperature change were reflected in time series patterns of the seasonal phenology indices. The spring thermal transition day of year tends to occur earlier in the year now compared to the late 1990s in all three ecoregions, but only the trend in the GOM was significant (Figure 3a, c, and e). In contrast, the autumn thermal transition day of the year trended to later days of the year in all three ecoregions and the trends were significant (Figure 3b, d, and f). The change in transition timing was over twice as many days in the GOM, where spring transition advanced by 12 d compared to a delay of the autumn transit by >26 d. In the GBK and MAB areas, spring advance was <10 d compared to autumn delay on at least 2 weeks. Hence, from 1997 to 2020, the timing of thermal events appears to be less impacted during the spring period and may be significantly delayed in the autumn period.

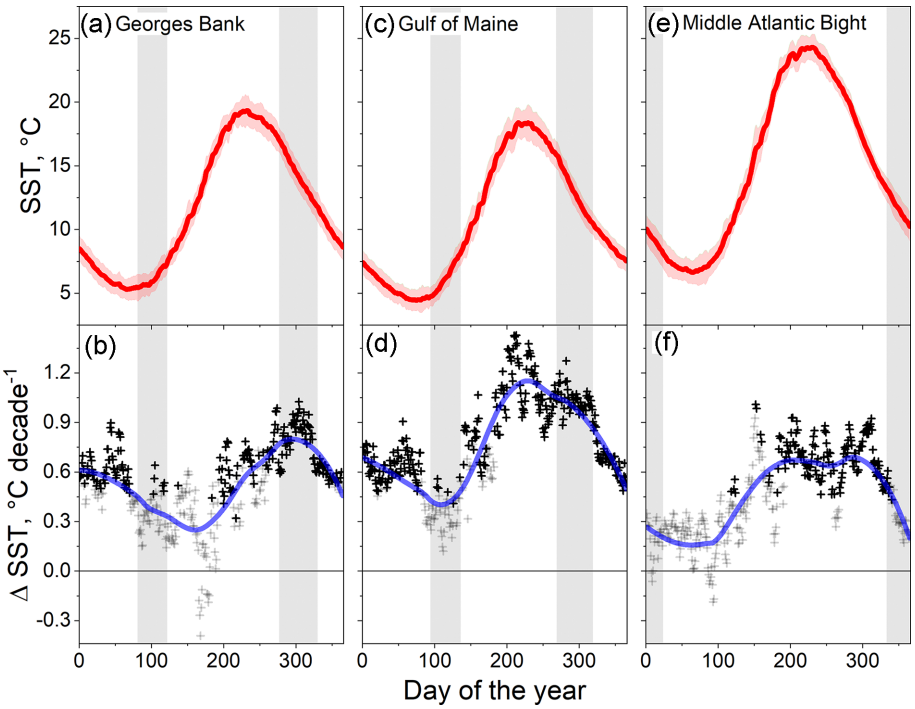

Figure 2. Mean SST, with standard deviation range shown in light red, by day of the year for the GBK (a), GOM (c), and MAB (e) ecoregions during 1997–2020. Change in SST as slopes by day of the year for the same ecoregions (b, d, f, respectively); significant slope ($p < 0.05$) marked with black "+", otherwise in grey. Blue curves are LOESS smoothers with tension factor of 0.5. Vertical grey-shaded bars mark mean start and duration of seasonal blooms (see Tables 1–3).

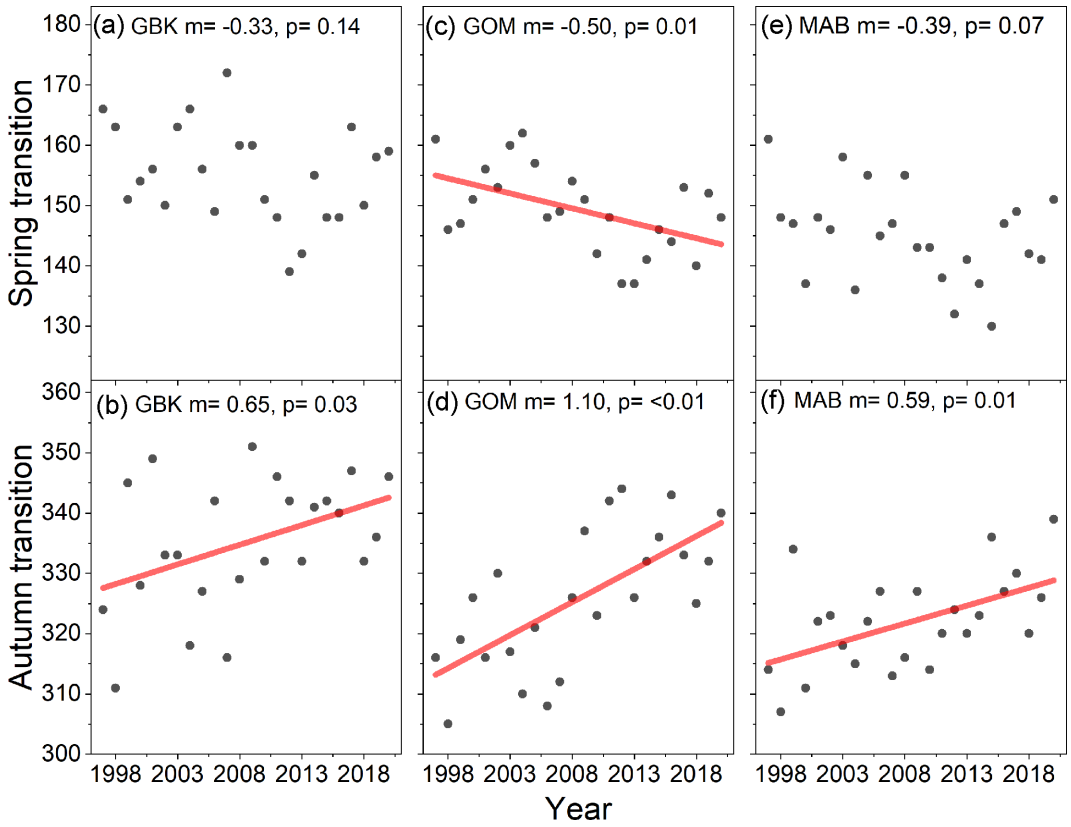

Figure 3. Spring thermal transition as day of the year for the GBK (a), GOM (c), and MAB (e) ecoregions during 1997–2020. Autumn transition for the same ecoregions (b, d, f, respectively). Theil–Sen slope and *p*-value for each scatter provided in the panel title; red lines are linear regressions ($p < 0.05$).

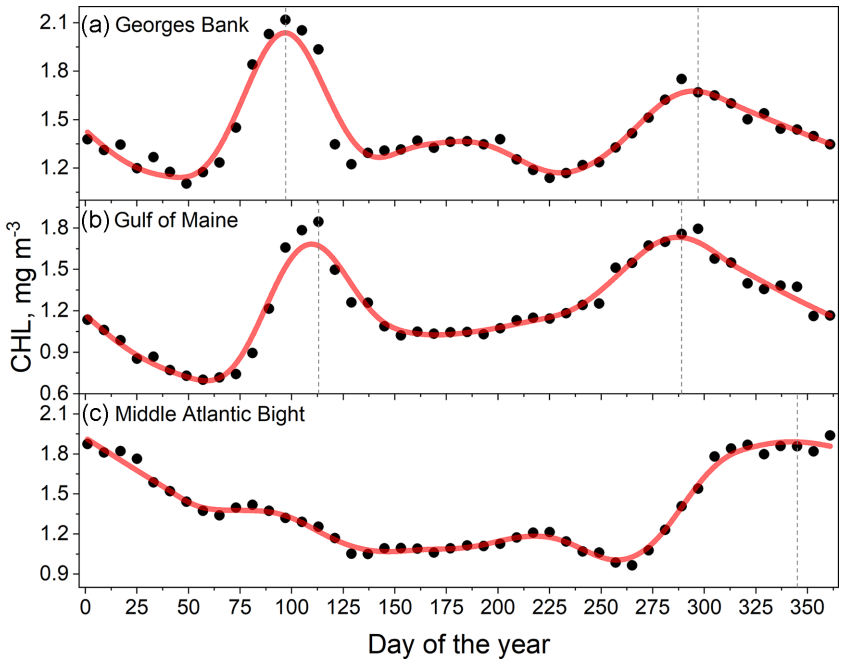

Figure 4. Mean CHL by day of the year for the GBK (a), GOM (b), and MAB (c) ecoregions. Red curves are LOESS smoothers with tension a factor of 0.25. Vertical dashed lines mark inflection points of the LOESS curves.

Change in bloom phenology

The annual climatology of CHL was used to identify seasonal bloom patterns that guided the analysis of bloom phenology. The CHL in the GBK ecoregion varied from seasonal lows of ∼1.1 mg m^{-3} to seasonal highs of 2.1 mg m^{-3} (Figure 4a), which spanned the range related to a spring and autumn blooms. The spring bloom was associated with a CHL maximum that typically occurred on 6 April (day of the year 97); hence, the search window for GBK spring blooms was set to 9 January (day of the year 9) so the mean CHL would be in the middle of the search window. The GBK autumn bloom typically occurred on 23 October (day of the year 297) and the search window set to 27 July (day of the year 209), accordingly. The GOM was also a two-bloom system, spanning a range of CHL of 0.69–1.74 mg m^{-3} (Figure 4b). The spring and autumn blooms for the period 1997–2020 were centred on 22 April (day of the year 113) and 15 October (day of the year 289), respectively; hence, the associated search windows started on 25 January through 19 July, days of the year 25 and 201, respectively.

Seasonal blooms were observable in most years in all three ecoregions. The spring bloom was observable in 20 of 23 years on GBK and in most years, there were multiple detections (Table 1). None of the bloom durations averaged more than nine 8-d periods, so all the data were included in the subsequent analysis. Similar to spring thermal transition timing, there were no discernible trends in either spring bloom start day or duration (Figure 5a and b). The autumn bloom was detected in 19 of 23 years; however, in two years, 2017–2018, the bloom duration averaged more than nine 8-d periods, hence, these years were excluded from the subsequent analysis. There were significant trends in bloom start date and duration of the GBK autumn bloom (Figure 5c and d). The autumn bloom started at around 20 September (day of the year 264) in early years and now tends to start around 23 October (day of the year 297). Autumn bloom duration was ∼7.5 weeks and is now ∼5 weeks long. Spring and autumn blooms were detected in the GOM in 20 and 19 of 23 years, respectively (Table 2). None of the detections of GOM blooms were eliminated due to bloom duration. Neither the spring nor autumn GOM bloom start day or duration contained any time series trends (Figure 6). The autumn bloom in the MAB was detected in 16 of 23 years and all blooms were of similar duration (Table 3). Neither the MAB bloom start day nor duration contained any time series trend (Figure 7). The only change in seasonal bloom phenology appears in the autumn bloom on GBK and there was no evidence of change in spring bloom timing or duration. In referencing back to SST (Figure 2b, d, and f), the mean bloom periods associated with spring blooms in GBK and GOM were dominated by modest and mostly non-significant rates of change, whereas the autumn bloom periods were associated with large and significant rates of change. The MAB bloom period was associated with non-significant rates of change.

Discussion

An asymmetry in temperature differentially affecting autumn conditions

Though it is well established that the NES is rapidly warming (Friedland *et al.*, 2020a; Pershing *et al.*, 2021), we demonstrated that the warming has not been seasonally uniform, with less temperature change in the spring. The thermal dynamics of the spring transition has not changed as much as the autumn transition. Likewise, and perhaps consequently, we observed little evidence for a change in spring bloom phenology. In contrast, the autumn bloom in the GBK ecoregion has become later and shorter, possibly due to more pronounced summer warming (Thomas *et al.*, 2017) that has changed destratification timing known to trigger autumn blooms. In

Table 1. Mean bloom start day of the year (Str) and bloom duration in the number of 8-d periods (Dur) for the GBK ecoregion in spring and autumn bloom periods.

	Spring					Autumn				
Year	Str	*SD*	Dur	*SD*	*N*	Str	*SD*	Dur	*SD*	*N*
1998	Non detection					281.9	12.4	8.4	3.1	27
1999	65.0	0.0	7.1	0.3	27	241.6	2.1	7.9	0.3	27
2000	74.5	3.2	4.0	0.4	22	276.0	4.0	5.2	0.6	21
2001	108.4	4.1	4.6	0.5	21	271.0	3.5	5.1	1.6	24
2002	81.0	12.0	8.3	4.0	9	261.4	4.1	6.5	1.4	27
2003	81.0	3.8	5.3	0.5	27	Non detection				
2004	89.0	0.0	4.3	0.5	18	276.3	4.0	7.3	1.8	27
2005	76.2	4.1	4.8	0.4	15	Non detection				
2006	70.3	11.3	4.3	1.4	18	273.0	0.0	6.7	0.5	21
2007	73.0	0.0	5.5	0.5	24	265.0	0.0	5.2	0.4	18
2008	78.3	10.2	5.4	1.2	27	305.0	0.0	4.0	0.0	9
2009	73.9	2.6	5.9	0.3	27	257.0	0.0	4.0	0.0	6
2010	85.0	7.1	5.9	1.2	24	273.0	0.0	4.5	0.5	27
2011	84.2	4.1	4.2	0.4	15	306.8	14.3	6.2	2.1	27
2012	81.0	0.0	4.0	0.0	15	289.9	9.0	6.9	1.1	27
2013	Non detection					289.0	0.0	4.6	0.8	16
2014	94.3	10.3	4.3	1.3	18	276.7	11.3	5.9	2.8	15
2015	79.4	3.3	5.2	0.4	15	278.3	7.7	6.2	1.3	27
2016	66.3	3.1	5.8	0.4	18	Non detection				
2017	97.0	0.0	4.0	0.0	9	*257.0*	*0.0*	*15.0*	*0.0*	*24*
2018	89.0	0.0	4.0	0.0	24	*273.9*	*6.0*	*12.8*	*0.7*	*27*
2019	Non detection					307.0	3.6	4.0	0.0	12
2020	78.3	3.8	4.5	1.3	27	Non detection				

Each mean reported with associated standard deviation (*SD*) and the number of blooms detected (*N*). Bloom means with a duration >9 indicated with italics.

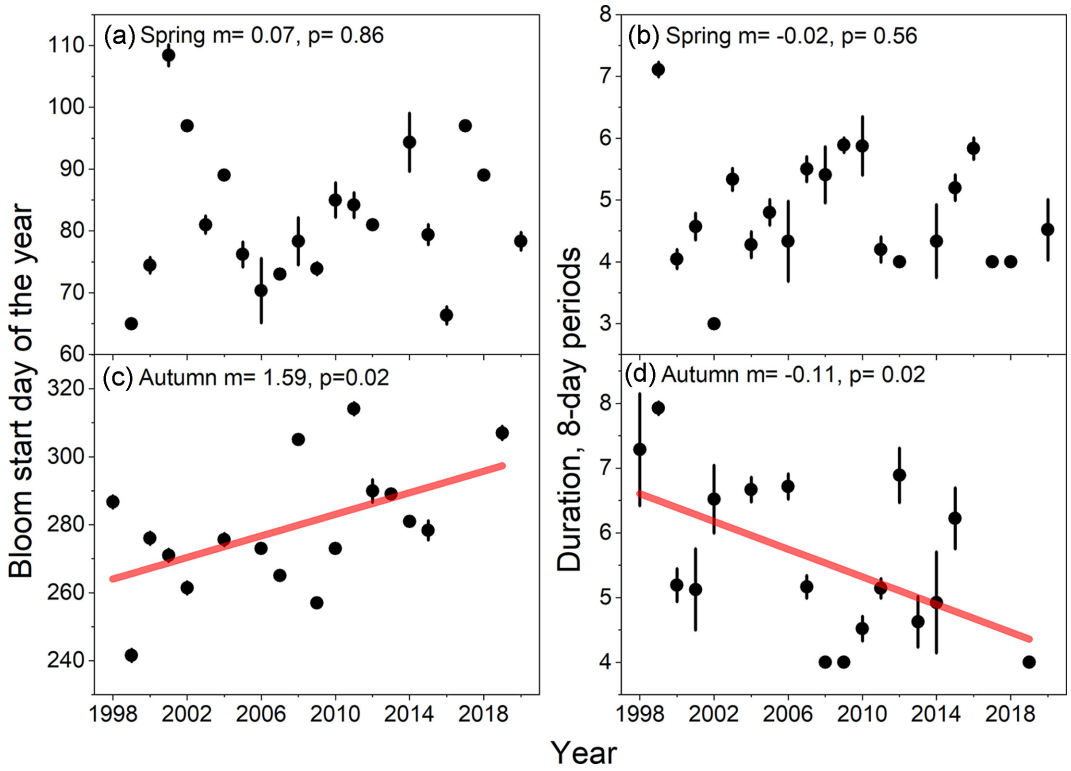

Figure 5. Time series of bloom start day of the year in the GBK ecoregion during spring (a) and autumn (c) and bloom duration for the same time periods (b, d, respectively). Theil–Sen slope and *p*-value for each scatter provided in the panel title; red lines are linear regressions ($p < 0.1$). Error bars are 95% *CIs*.

the GOM, we also have the ability to consider a long-term and high-resolution *in-situ* sampling program called the GOM North Atlantic Time Series or GNATS (Balch *et al.*, 2012). GNATS data demonstrate that surface waters have warmed significantly in summer, fall, and winter between 1998 and 2018; however, during spring months, the surface waters showed a significant cooling trend when averaged across the GOM, corroborating the seasonal asymmetry also observed

Table 2. Mean bloom start day of the year (Str) and bloom duration in the number of 8-d periods (Dur) for the GOM ecoregion in spring and autumn bloom periods.

	Spring					Autumn				
Year	Str	*SD*	Dur	*SD*	*N*	Str	*SD*	Dur	*SD*	*N*
1998	81.0	0.0	6.3	0.5	16	291.9	15.5	8.2	2.1	22
1999	98.8	3.4	4.3	0.5	27	265.0	0.0	8.5	0.5	18
2000	Non detection					279.0	3.6	4.0	0.7	12
2001	81.0	0.0	6.6	1.9	27	265.0	0.0	6.0	0.0	9
2002	105.0	0.0	5.1	0.3	27	246.3	3.8	6.2	0.8	27
2003	99.0	3.5	5.1	0.4	24	261.8	4.1	8.6	0.5	15
2004	105.0	0.0	3.7	0.4	27	247.2	11.4	6.0	1.8	27
2005	Non detection					245.4	7.8	5.4	1.0	27
2006	81.0	0.0	5.0	0.0	15	259.7	3.8	4.7	0.5	27
2007	89.0	0.0	8.1	0.3	27	264.1	6.0	5.4	0.7	27
2008	83.7	3.8	6.6	0.5	27	273.0	0.0	8.0	0.0	3
2009	90.3	3.1	5.2	0.4	18	251.2	3.7	5.7	0.5	25
2010	89.0	0.0	5.5	1.9	18	250.1	2.9	7.9	0.4	21
2011	89.0	0.0	4.8	1.3	24	297.0	0.0	8.0	0.0	3
2012	79.0	3.5	4.5	0.7	24	284.2	4.0	5.6	1.2	25
2013	Non detection					290.1	2.9	5.9	1.9	21
2014	97.0	0.0	4.2	0.4	18	267.7	3.8	5.4	0.5	27
2015	94.3	3.9	5.6	1.0	18	Non detection				
2016	105.0	0.0	5.1	0.6	19	282.8	3.4	5.6	0.5	27
2017	97.0	0.0	4.0	0.0	24	Non detection				
2018	89.0	0.0	4.2	0.6	27	Non detection				
2019	121.0	0.0	7.5	0.5	18	265.0	9.4	6.9	1.6	27
2020	109.0	4.4	4.5	0.5	6	Non detection				

Each mean reported with associated standard deviation (*SD*) and the number of blooms detected (*N*).

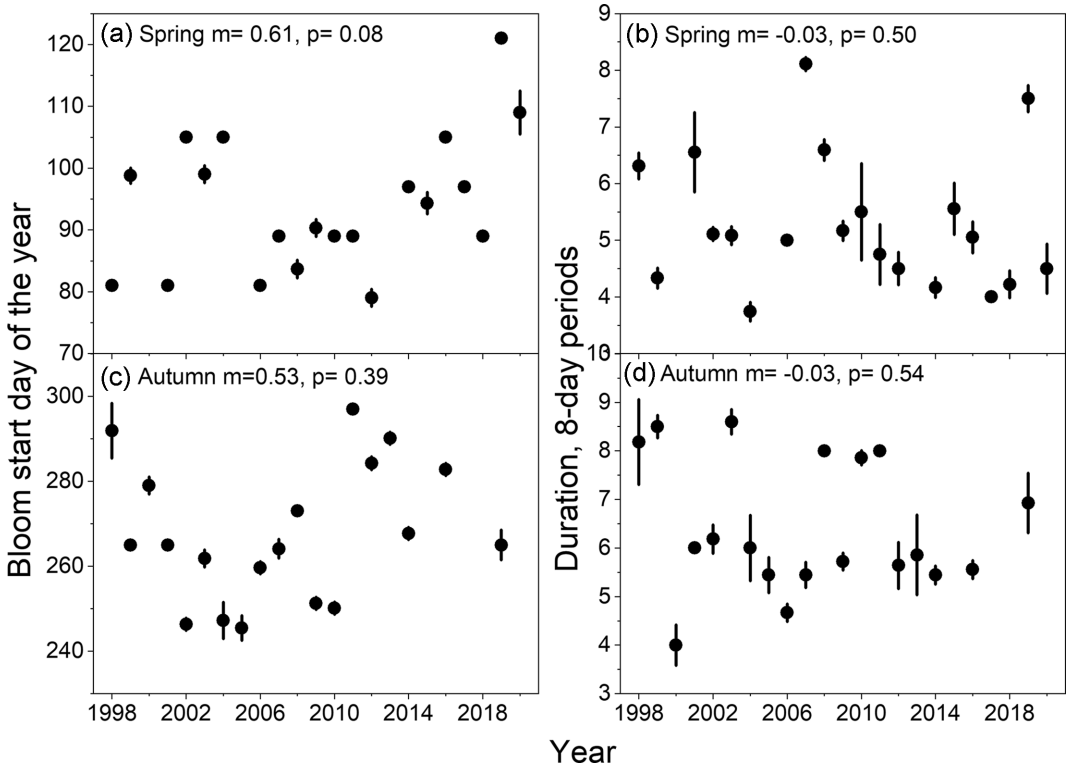

Figure 6. Time series of bloom start day of the year in the GOM ecoregion during spring (a) and autumn (c) and bloom duration for the same time periods (b, d, respectively). Theil–Sen slope and *p*-value for each scatter provided in the panel title. Error bars are 95% *CIs*.

in the remote sensing data (Balch *et al.*, 2022). A logical progression would be to examine stratification dynamics with respect to specific bloom events and determine, at least for the autumn period on GBK, whether the stratification phenology associated with the thermal phenology in the surface waters has changed. This daunting task would require regional *in-situ* data collected seasonally, over spatially varying sample locations; but perhaps future work could use model reconstruc-

Table 3. Mean bloom start day of the year (Str) and bloom duration in the number of 8-d periods (Dur) for the MAB ecoregion in the autumn bloom period.

Year	Str	*SD*	Dur	*SD*	*N*
1997	353.0	0.0	5.4	0.5	21
1998	*317.0*	*4.2*	*7.5*	*0.5*	*12*
1999	Non detection				
2000	335.0	5.4	8.5	0.7	24
2001	313.0	0.0	8.0	0.0	25
2002	Non detection				
2003	337.0	0.0	8.0	0.0	3
2004	329.0	36.7	4.6	1.0	27
2005	297.0	0.0	9.0	0.0	3
2006	Non detection				
2007	377.8	22.8	5.1	1.4	10
2008	Non detection				
2009	345.0	8.2	5.8	0.9	18
2010	321.0	0.0	9.0	0.0	3
2011	Non detection				
2012	323.7	6.1	6.7	0.8	18
2013	Non detection				
2014	Non detection				
2015	352.0	2.7	5.4	0.7	24
2016	348.4	8.6	8.6	1.1	21
2017	332.2	6.6	7.0	1.1	15
2018	313.0	0.0	6.0	0.0	3
2019	329.0	0.0	9.0	0.0	3

Each mean reported with associated standard deviation (*SD*) and the number of blooms detected (*N*).

tions of temperature at a depth that are becoming increasingly more reliable in terms of bias corrections (du Pontavice *et al.*, 2022).

Basin scale effects on SST and CHL

Considerable attention has been focused on temperature changes in the NES and the factors at play (Kavanaugh *et al.*, 2017), but these changes must be delineated by those occurring in the surface layer vs. those changes to the benthos. While both surface and bottom water temperatures are increasing, there is evidence that they are doing so differentially (Friedland *et al.*, 2020a; Record *et al.*, 2019a). Temperature change in bottom waters of the NES appear to be driven by the advection of different water masses associated with Gulf Stream dynamics (Gonçalves Neto *et al.*, 2021). Surface water temperature appears to be more influenced by basin scale drivers of atmospheric circulation, including the weakening of the Atlantic Meridional Overturning Circulation and continued positive phase of the North Atlantic Oscillation (Karmalkar and Horton, 2021). Persistent warming or heat waves thus develop in the NES depending on the latitudinal position of the jet stream (Perez *et al.*, 2021). The seasonal excursion of summer continental temperature is beyond that observed during winter, hence, the warming asymmetry we observe in the surface layer of the NES.

Beyond thermal effects, differences in water mass nutrient content have implications for productivity; the cool, fresher Labrador slope origin water contains higher nutrient levels than warmer, saltier Atlantic slope water (Townsend *et al.*, 2015). In parallel to the step change increase in surface water temperature throughout most of the NES, the accompanied change in nutrient loading would support an observed drop in GOM primary productivity (Balch *et al.*, 2012, 2022). Interestingly, NES CHL has shown a linear decline rather than a step change on the NES (Friedland *et al.*, 2020b). This gradual decline may be consistent with a more conservative decline in nutrients in the system; hence, it suggests the possibility that with each production year, more of the nutrients incorporated by phytoplankton have been sequestered from the system via the burial of particulates or migration of particulates off the continental shelf.

Absence of a spring bloom effect

Many NES organisms, including those of commercial importance, time their reproductive processes to the spring phytoplankton bloom. Despite significant warming of the ecosystem, we did not detect any long-term change in spring bloom timing or duration. It is well established that increasing temperature will increase the growth rates of marine phytoplankton (Trombetta *et al.*, 2019) and warming has been found to be one of the principal agents triggering spring blooms (Almén and Tamelander, 2020). In more northerly systems, direct thermal effects can be superseded by the modulating effects of sea ice retreat (Dong *et al.*, 2020) and stratification that results in shallower surface layer mixing. But also at higher latitudes, in systems without ice, spring bloom timing was found to be without trend, though interannual variability was impacted by physical factors such as temperature and mixed layer depth

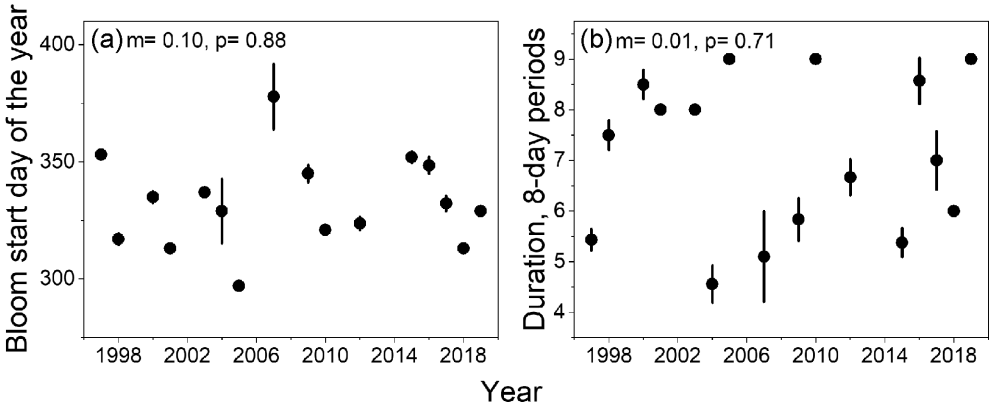

Figure 7. Time series of bloom start day of the year in the MAB ecoregion during autumn (a) and bloom duration for the same time period (b). Theil–Sen slope and *p*-value for each scatter provided in the panel title. Error bars are 95% *CIs*.

(Silva *et al.*, 2021). However, it is important to be mindful of the range of other factors that can influence bloom timing including light limitation, nutrient supply, and grazing impacts.

Evidence for light limitation is available in both laboratory trials and natural experiments. Mesocosm experiments show that spring bloom timing may be impacted more by light than accelerated warming, especially as photosynthetically active radiation becomes more available during the spring (Sommer and Lengfellner, 2008). In the North Sea, delayed spring bloom timing was related to water clarity, where greater turbidity resulted in delayed blooms (Opdal *et al.*, 2019). In the Labrador Sea, the regional differences in seasonal shoaling appears to control spring bloom formation, which would be consistent with mixed layer effects on light exposure (Marchese *et al.*, 2019). In the GOM, the absorption of light by river-supplied, coloured dissolved organic matter (CDOM) can also induce light limitation of phytoplankton productivity by the absorption of blue wavelengths by humic material, thus slowing phytoplankton growth (Balch *et al.*, 2012). Moreover, there is asymmetry in the discharge of CDOM from GOM watersheds, with more blue-absorbing, humic-rich, CDOM discharged during autumn freshets, while spring runoff is less absorbing to light used by phytoplankton for photosynthesis.

The nutrient supply for the development of the spring bloom is in part dependent on the rate of spring mixed layer development and the origin and composition of source water entering the ecosystem. The depletion of nutrients in water masses destined to enter the NES is known to impact on bloom timing (Ji *et al.*, 2007). Water masses entering the NES have differing nitrate and silicate concentrations, not always recognizable from temperature and salinity characteristics alone, but can be generalized by either cold northern source water or warm source water associated with the Gulf Stream (Townsend *et al.*, 2015). Variation in bloom development may be related to the variability in key nutrients and their stoichiometric ratios within these dominant water masses.

Top-down control on bloom formation and duration may play a prominent role in the NES ecosystem. A growing body of evidence illustrates how decoupled zooplankton grazing can initiate bloom formation (Rohr *et al.*, 2017), control bloom duration (Kauko *et al.*, 2021), and shape long-term bloom phenology trends (Guinder *et al.*, 2017). The copepod *Calanus finmarchicus* emerges from diapause in the GOM relying in part on thermal triggers, and may shape the phenology of the autumn bloom on the GOM (Ji *et al.*, 2021). The taxon is less abundant on GBK where there is a stronger signal in bloom phenology. While the copepod, *Centropages typicus*, has been a dominant taxon in the MAB, its centre of peak abundance have changed both spatially and temporally, which could affect its role in shaping bloom dynamics (Morse *et al.*, 2017). Efforts to model NES bloom dynamics underscore the need for better information of the distribution and abundance of grazing animals (Zang *et al.*, 2021).

Food web ramifications

Fisheries production on the US Northeast Continental Shelf Ecosystem is mainly dependent upon the primary production of phytoplankton communities, which also defines the habitat extent of many key species (Friedland *et al.*, 2021). In some ecosystems, fisheries production can be traced to allochthonous energy sources such as terrestrial vegetation, but these are relatively minor contributions in the NES (Zinkann *et al.*, 2021). The trophic pathways fed by phytoplankton tend to fall within two main paradigms. The first paradigm is governed by the utilization of pelagic productivity directly through pelagic food webs, classically viewed as energy flow from phytoplankton to zooplankton to fish (MacKenzie *et al.*, 2019). In the second, fisheries production is the result of particulate organic carbon flux from pelagic productivity to the benthos, and then into demersal food webs (Stock *et al.*, 2017). Considering these two pathways, measurements associated with primary productivity take on different meanings depending on which food web is considered. While the rate of primary productivity is associated with the rate of fixed carbon entering pelagic food webs, chlorophyll as a metric representing phytoplankton biomass may be a better indicator of organic carbon flux to the benthos. Interestingly, these production metrics—primary productivity and CHL—are not always correlated because CHL blooms are often temporally separated from the maxima of primary productivity. Hence, in considering the phytoplankton communities of the shelf ecosystem, it is useful to consider the distribution of both primary productivity and chlorophyll concentration in time and space.

With these factors in mind, we examined the potential ramifications of changing autumn bloom phenology, since we see little evidence of changing spring bloom phenology. The autumn bloom on GBK has been associated with the recruitment of higher trophic level organisms such as haddock (Leaf and Friedland, 2014). In this case, a shift to an earlier and longer bloom would likely increase fish recruitment; however, a later and shorter duration bloom would have the opposite effect. In considering food web processes, shorter bloom periods would be expected to decrease prey availability to zooplankton taxa such as *Centropages* spp., thus impairing trophic transfer associated with the production of the autumn bloom (Steele *et al.*, 2007).

Consequences for species distribution

Climate change in marine ecosystems is frequently framed in the context of poleward shifts. For example, "Tropicalization" describes the poleward shift of environmental conditions and associated species from tropical to temperate environments (Kleisner *et al.*, 2016). If the temperature range over a season is considered an important environmental property unto itself, then the NES is becoming less tropical, with a greater difference between summer and winter temperatures.

From the perspective of species' thermal niches, the upper temperature bound constrains the poleward side of the range, so warming summers should allow northward expansion, something that has been observed across many taxa, particularly in the GOM (Kleisner *et al.*, 2016). The lower bounding temperature constrains the equatorward thermal range, so the absence of warming winters could maintain the southern limit of some species, preventing the poleward shift at the equator edge of the range. For some subarctic species, such as the key copepod *C. finmarchicus*, persistence has been observed to some degree in the western GOM despite a warming trend, due to a combination of the persistence of spring bloom dynamics and the overwintering habitat (Runge *et al.*, 2015).

At a first estimation, the geographic widening of thermal ranges has the potential to increase species overlap, interaction, and diversity. However, seasonal changes can have more

nuanced consequences for species with seasonally dynamic life histories. For many species, phenological dynamics and their relationship with life history requirements can outweigh any straightforward relationship with a species' thermal envelope. The high amplitude seasonality of conditions in the GOM, in particular, means that the seasonal accumulation of energy stores such as lipids are a foundational organizing feature of the system (Pershing and Stamieszkin, 2020). In such cases, the properties of seasonal cycles are just as crucial as temperature in setting the structure of the ecosystem (Record *et al.*, 2018). Many climate projections focus on shifts in temperature as a means of predicting future ecosystem states (Pershing *et al.*, 2021). With shifts in seasonality working in asymmetrical ways, counter to shifts in temperature, concepts like tropicalization and climate velocity might not describe the coming changes adequately.

Consequences for protected species

Seasonal asymmetry has additional consequences for protected species, especially for those exhibiting phenological changes and poleward distributional shifts. The case of North Atlantic right whale (*Eubalaena glacialis*) offers an illustrative example. Protective measures (e.g. restrictions on fishing and shipping) designed to eliminate human-induced injury and death to right whales are based upon the species' migratory phenology. Over the past one to two decades, right whale abundance in the southwestern GOM in winter and spring has increased (O'Brien *et al.*, 2022) and peak-habitat use in this region occurs almost 3 weeks later (Pendleton *et al.*, 2022). Similarly, abundance in the summer and autumn has shifted to a novel habitat north of the GOM—the Gulf of St. Lawrence (Crowe *et al.*, 2021). This northward expansion of right whales has almost certainly result in decreased abundance within historic feeding grounds in the eastern GOM. This asymmetric expansion of habitat—stable yet increasing habitat-use in the south during winter/spring while expanding to the north in summer/autumn—is reflective of the thermal asymmetry described here. Right whales must find and consume ultra-dense concentrations of zooplankton, generally *Pseudocalanus* spp., *Centropages typicus*, and to some extent *C. finmarchicus*, in the winter and spring, and *C. finmarchicus* in the late summer and fall (Pendleton *et al.*, 2009; Mayo and Marx, 2011). Persistence of right whales in the southwestern GOM is likely due to enhanced production of small copepods in the southwestern GOM during spring. While, the northward expansion of right whales may be due to warming waters in the GOM that have reduced the supply and altered the life-history of late-stage *C. finmarchicus* that right whales were known to target during autumn in the eastern GOM (Record *et al.*, 2019a). To respond to these changes, US state managers have expanded protections (MADMF, 2021), while federal managers have continued to issue spatiotemporally dynamic vessel slowdown zones (NOAA, 2008). In Canada, the unexpected arrival of large numbers of right whales into the Gulf of St. Lawrence resulted in many whale mortalities, as protections were not in place (Davies *et al.*, 2019), and managers responded by closing (and later reopening) entire fisheries. This is one example of an unexpected challenge that resource managers face, partially due to asymmetric thermal and productivity phenology, as they balance societal needs with preserving an endangered species.

Acknowledgements

We thank anonymous reviewers for their comments, who have greatly improved the manuscript. Support for WMB was provided by NASA (NNX17A177G, 80NSSC22K165 and NSSC21K1748).

Conflict of interest statement

The authors declare that they have no known competing financial interests or personal relationships that could have appeared to influence the work reported in this paper.

Data availability statement

Sea surface temperature data were from the OISST dataset at https://www.ncdc.noaa.gov/oisst/optimum-interpolation-sea-surface-temperature-oisst-v21. Chlorophyll concentration data were from the Hermes GlobColour website: http://hermes.acri.fr/.

Author contributions

K.F. and N.R. contributed to the conception of the paper and its figures, and led the writing of the paper. All other authors contributed to writing and editing the manuscript and approved the final draft.

References

Almén, A-K., and Tamelander, T. 2020. Temperature-related timing of the spring bloom and match between phytoplankton and zooplankton. Marine Biology Research, 16: 674–682.

Asch, R. G., Stock, C. A., and Sarmiento, J. L. 2019. Climate change impacts on mismatches between phytoplankton blooms and fish spawning phenology. Global Change Biology, 25: 2544–2559.

Balch, W. M., Drapeau, D. T., Bowler, B. C., and Huntington, T. G. 2012. Step-changes in the physical, chemical and biological characteristics of the Gulf of Maine, as documented by the GNATS time series. Marine Ecology Progress Series, 450: 11–35.

Balch, W. M., Drapeau, D. T., Bowler, B. C., Record, N. R., Bates, N. R., Pinkham, S., Garley, R., *et al.* 2022. Changing hydrographic, biogeochemical, and acidification properties in the Gulf of Maine as measured by the Gulf of Maine North Atlantic time series, GNATS, between 1998 and 2018. Journal of Geophysical Research: Biogeosciences, 127: e2022JG006790.

Chen, Z. M., Curchitser, E., Chant, R., and Kang, D. J. 2018. Seasonal variability of the cold pool over the Mid-Atlantic Bight continental shelf. Journal of Geophysical Research: Oceans, 123: 8203–8226.

Cohen, J. L., Furtado, J. C., Barlow, M., Alexeev, V. A., and Cherry, J. E. 2012. Asymmetric seasonal temperature trends. Geophysical Research Letters, 39: L04705.

Crowe, L. M., Brown, M. W., Corkeron, P. J., Hamilton, P. K., Ramp, C., Ratelle, S., Vanderlaan, A. S. M., *et al.* 2021. In plane sight: a mark-recapture analysis of North Atlantic right whales in the Gulf of St. Lawrence. Endangered Species Research, 46: 227–251.

Davies, K. T. A., Brown, M. W., Hamilton, P. K., Knowlton, A. R., Taggart, C. T., and Vanderlaan, A. S. M. 2019. Variation in North Atlantic right whale *Eubalaena glacialis* occurrence in the Bay of Fundy, Canada, over three decades. Endangered Species Research, 39: 159–171.

Dong, K., Kvile, K. Ø., Stenseth, N. C., and Stige, L. C. 2020. Associations among temperature, sea ice and phytoplankton bloom dynamics in the Barents Sea. Marine Ecology Progress Series, 635: 25–36.

du Pontavice, H., Miller, T. J., Stock, B. C., Chen, Z., and Saba, V. S. 2022. Ocean model-based covariates improve a marine fish stock

assessment when observations are limited. ICES Journal of Marine Science, 79: 1259–1273.
Friedland, K. D. 2021. A test of the provisioning hypothesis of recruitment control in Georges Bank haddock. Canadian Journal of Fisheries and Aquatic Sciences, 78: 655–658.
Friedland, K. D., Bachman, M., Davies, A., Frelat, R., McManus, M. C., Morse, R., Pickens, B. A., *et al.* 2021. Machine learning highlights the importance of primary and secondary production in determining habitat for marine fish and macroinvertebrates. Aquatic Conservation: Marine and Freshwater Ecosystems, 31: 1482–1498.
Friedland, K. D., and Hare, J. A. 2007. Long-term trends and regime shifts in sea surface temperature on the continental shelf of the northeast United States. Continental Shelf Research, 27: 2313–2328.
Friedland, K. D., Leaf, R. T., Kane, J., Tommasi, D., Asch, R. G., Rebuck, N., Ji, R., *et al.* 2015a. Spring bloom dynamics and zooplankton biomass response on the US Northeast Continental Shelf. Continental Shelf Research, 102: 47–61.
Friedland, K. D., Leaf, R. T., Kristiansen, T., and Large, S. I. 2015b. Layered effects of parental condition and larval survival on the recruitment of neighboring haddock stocks. Canadian Journal of Fisheries and Aquatic Sciences, 72: 1672–1681.
Friedland, K. D., Morse, R. E., Manning, J. P., Melrose, D. C., Miles, T., Goode, A. G., Brady, D. C., *et al.* 2020a. Trends and change points in surface and bottom thermal environments of the US Northeast Continental Shelf Ecosystem. Fisheries Oceanography, 29: 396–414.
Friedland, K. D., Morse, R. E., Shackell, N., Tam, J. C., Morano, J. L., Moisan, J. R., and Brady, D. C. 2020b. Changing physical conditions and lower and upper trophic level responses on the US Northeast Shelf. Frontiers in Marine Science, 7: 567445.
Friedland, K. D., Record, N. R., Asch, R. G., Kristiansen, T., Saba, V. S., Drinkwater, K. F., Henson, S., *et al.* 2016. Seasonal phytoplankton blooms in the North Atlantic linked to the overwintering strategies of copepods. Elementa: Science of the Anthropocene, 4: 000099.
Gordon, H. R., and McCluney, W. R. 1975. Estimation of the depth of sunlight penetration in the sea for remote sensing. Applied Optics, 14: 413–416.
Guinder, V. A., Molinero, J. C., López Abbate, C. M., Berasategui, A. A., Popovich, C. A., Spetter, C. V., Marcovecchio, J. E., *et al.* 2017. Phenological changes of blooming diatoms promoted by compound bottom-up and top-down controls. Estuaries and Coasts, 40: 95–104.
Hardison, S., Perretti, C. T., DePiper, G. S., and Beet, A. 2019. A simulation study of trend detection methods for integrated ecosystem assessment. ICES Journal of Marine Science, 76: 2060–2069.
Henson, S. A., Cole, H. S., Hopkins, J., Martin, A. P., and Yool, A. 2018. Detection of climate change-driven trends in phytoplankton phenology. Global Change Biology, 24: e101–e111.
Hjerne, O., Hajdu, S., Larsson, U., Downing, A. S., and Winder, M. 2019. Climate driven changes in timing, composition and magnitude of the Baltic Sea phytoplankton spring bloom. Frontiers in Marine Science, 6: 482.
Hunter-Cevera, K. R., Neubert, M. G., Olson, R. J., Solow, A. R., Shalapyonok, A., and Sosik, H. M. 2016. Physiological and ecological drivers of early spring blooms of a coastal phytoplankter. Science, 354: 326–329.
Ji, R., Runge, J. A., Davis, C. S., and Wiebe, P. H. 2021. Drivers of variability of *Calanus finmarchicus* in the Gulf of Maine: roles of internal production and external exchange. ICES Journal of Marine Science, 79: 775–784.
Ji, R. B., Davis, C. S., Chen, C. S., Townsend, D. W., Mountain, D. G., and Beardsley, R. C. 2007. Influence of ocean freshening on shelf phytoplankton dynamics. Geophysical Research Letters, 34: L24607.
Karmalkar, A. V., and Horton, R. M. 2021. Drivers of exceptional coastal warming in the northeastern United States. Nature Climate Change, 11: 854–860.
Kauko, H. M., Hattermann, T., Ryan-Keogh, T., Singh, A., de Steur, L., Fransson, A., Chierici, M., *et al.* 2021. Phenology and environmental control of phytoplankton blooms in the Kong Håkon VII Hav in the Southern Ocean. Frontiers in Marine Science, 8: 287.
Kavanaugh, M. T., Rheuban, J. E., Luis, K. M. A., and Doney, S. C. 2017. Thirty-three years of ocean benthic warming along the US Northeast Continental Shelf and slope: patterns, drivers, and ecological consequences. Journal of Geophysical Research: Oceans, 122: 9399–9414.
Kleisner, K. M., Fogarty, M. J., McGee, S., Barnette, A., Fratantoni, P., Greene, J., Hare, J. A., *et al.* 2016. The effects of sub-regional climate velocity on the distribution and spatial extent of marine species assemblages. PLoS ONE, 11: e0149220.
Kodama, T., Wagawa, T., Ohshimo, S., Morimoto, H., Iguchi, N., Fukudome, K-I., Goto, T., *et al.* 2018. Improvement in recruitment of Japanese sardine with delays of the spring phytoplankton bloom in the Sea of Japan. Fisheries Oceanography, 27: 289–301.
Kristiansen, T., Drinkwater, K. F., Lough, R. G., and Sundby, S. 2011. Recruitment variability in North Atlantic Cod and match–mismatch dynamics. PLoS One, 6: e17456.
Leaf, R. T., and Friedland, K. D. 2014. Autumn bloom phenology and magnitude influence haddock recruitment on Georges Bank. ICES Journal of Marine Science, 71: 2017–2025.
Li, Y., Wang, Q., Li, Q., Liu, Y., and Wang, Y. 2021. An asymmetric variation of hot and cold SST extremes in the China Seas during the recent warming hiatus period. Scientific Reports, 11: 2014.
MacKenzie, K. M., Robertson, D. R., Adams, J. N., Altieri, A. H., and Turner, B. L. 2019. Structure and nutrient transfer in a tropical pelagic upwelling food web: from isoscapes to the whole ecosystem. Progress in Oceanography, 178: 102145.
MADMF. 2021. Massachusetts Division of Marine Fisheries. 322 CMR 12.00: Protected Species. https://www.mass.gov/regulations/322-CMR-1200-protected-species. (last accessed date January 1, 2023).
Marchese, C., Castro de la Guardia, L., Myers, P. G., and Bélanger, S. 2019. Regional differences and inter-annual variability in the timing of surface phytoplankton blooms in the Labrador Sea. Ecological Indicators, 96: 81–90.
Maritorena, S., d'Andon, O. H. F., Mangin, A., and Siegel, D. A. 2010. Merged satellite ocean color data products using a bio-optical model: characteristics, benefits and issues. Remote Sensing of Environment, 114: 1791–1804.
Mayo, C. A., and Marx, M. K. 2011. Surface foraging behaviour of the North Atlantic right whale, *Eubalaena glacialis*, and associated zooplankton characteristics. Canadian Journal of Zoology, 68: 2214–2220.
Morse, R. E., Friedland, K. D., Tommasi, D., Stock, C., and Nye, J. 2017. Distinct zooplankton regime shift patterns across ecoregions of the US Northeast continental shelf large marine ecosystem. Journal of Marine Systems, 165: 77–91.
Neto, G. A., Langan, A. J., and Palter, J. B. 2021. Changes in the Gulf Stream preceded rapid warming of the Northwest Atlantic Shelf. Communications Earth & Environment, 2: 1–10.
NOAA. 2008. Endangered fish and wildlife; final rule to implement speed restrictions to reduce the threat of ship collisions with North Atlantic right whales. Federal Register, 73:60173–60191.
O'Brien, O., Pendleton, D. E., Ganley, L. C., McKenna, K. R., Kenney, R. D., Quintana-Rizzo, E., Mayo, C. A., *et al.* 2022. Repatriation of a historical North Atlantic right whale habitat during an era of rapid climate change. Scientific Reports, 12: 12407.
Opdal, A. F., Lindemann, C., and Aksnes, D. L. 2019. Centennial decline in North Sea water clarity causes strong delay in phytoplankton bloom timing. Global Change Biology, 25: 3946–3953.
Pendleton, D. E., Pershing, A. J., Brown, M. W., Mayo, C. A., Kenney, R. D., Record, N. R., and Cole, T. V. N. 2009. Regional-scale mean copepod concentration indicates relative abundance of North Atlantic right whales. Marine Ecology Progress Series, 378: 211–225.
Pendleton, D. E., Tingley, M. W., Ganley, L. C., Friedland, K. D., Mayo, C., Brown, M. W., McKenna, B. E., *et al.* 2022. Decadal-scale phenology and seasonal climate drivers of migratory baleen whales in a rapidly warming marine ecosystem. Global Change Biology, 28: 4989–5005.

Perez, E., Ryan, S., Andres, M., Gawarkiewicz, G., Ummenhofer, C. C., Bane, J., and Haines, S. 2021. Understanding physical drivers of the 2015/16 marine heatwaves in the Northwest Atlantic. Scientific Reports, 11: 17623.

Pershing, A. J., Alexander, M. A., Brady, D. C., Brickman, D., Curchitser, E. N., Diamond, A. W., McClenachan, L., *et al.* 2021. Climate impacts on the Gulf of Maine ecosystem: a review of observed and expected changes in 2050 from rising temperatures. Elementa: Science of the Anthropocene, 9: 00076. https://doi.org/10.1525/elementa.2020.00076

Pershing, A. J., Alexander, M. A., Hernandez, C. M., Kerr, L. A., Le Bris, A., Mills, K. E., Nye, J. A., *et al.* 2015. Slow adaptation in the face of rapid warming leads to collapse of the Gulf of Maine cod fishery. Science, 350: 809–812.

Pershing, A. J., and Stamieszkin, K. 2020. The North Atlantic ecosystem, from plankton to whales. Annual Review of Marine Science, 12: 339–359.

Record, N. R., Balch, W. M., and Stamieszkin, K. 2019b. Century-scale changes in phytoplankton phenology in the Gulf of Maine. PeerJ, 7: e6735.

Record, N. R., Ji, R., Maps, F., Varpe, Ø., Runge, J. A., Petrik, C. M., and Johns, D. 2018. Copepod diapause and the biogeography of the marine lipidscape. Journal of Biogeography, 45: 2238–2251.

Record, N. R., Kenney, R., Balch, W., Davies, K., Pershing, A., Johnson, C., Stamieszkin, K., *et al.* 2019a. Rapid climate-driven circulation changes threaten conservation of endangered North Atlantic right whales. Oceanography, 32: 162–169.

Reynolds, R. W., Smith, T. M., Liu, C., Chelton, D. B., Casey, K. S., and Schlax, M. G. 2007. Daily high-resolution-blended analyses for sea surface temperature. Journal of Climate, 20: 5473–5496.

Rodionov, S. N. 2006. Use of prewhitening in climate regime shift detection. Geophysical Research Letters, 33: 1–4.

Rohr, T., Long, M. C., Kavanaugh, M. T., Lindsay, K., and Doney, S. C. 2017. Variability in the mechanisms controlling Southern Ocean phytoplankton bloom phenology in an ocean model and satellite observations. Global Biogeochemical Cycles, 31: 922–940.

Runge, J. A., Ji, R. B., Thompson, C. R. S., Record, N. R., Chen, C. S., Vandemark, D. C., Salisbury, J. E., *et al.* 2015. Persistence of *Calanus finmarchicus* in the western Gulf of Maine during recent extreme warming. Journal of Plankton Research, 37: 221–232.

Sedwick, P. N., Bernhardt, P. W., Mulholland, M. R., Najjar, R. G., Blumen, L. M., Sohst, B. M., Sookhdeo, C., *et al.* 2018. Assessing phytoplankton nutritional status and potential impact of wet deposition in seasonally oligotrophic waters of the Mid-Atlantic Bight. Geophysical Research Letters, 45: 3203–3211.

Sherman, K., Jaworski, N. A., and Smayda, T. J. 1996. The Northeast Shelf Ecosystem: assessment, sustainability, and management. Blackwell Science, Cambridge, MA. 564 p.

Silva, E., Counillon, F., Brajard, J., Korosov, A., Pettersson, L. H., Samuelsen, A., and Keenlyside, N. 2021. Twenty-one years of phytoplankton bloom phenology in the Barents, Norwegian, and North Seas. Frontiers in Marine Science, 8: 1626.

Sommer, U., and Lengfellner, K. 2008. Climate change and the timing, magnitude, and composition of the phytoplankton spring bloom. Global Change Biology, 14: 1199–1208.

Song, H. J., Ji, R. B., Stock, C., Kearney, K., and Wang, Z. L. 2011. Interannual variability in phytoplankton blooms and plankton productivity over the Nova Scotian Shelf and in the Gulf of Maine. Marine Ecology Progress Series, 426: 105–118.

Song, H. J., Ji, R. B., Stock, C., and Wang, Z. L. 2010. Phenology of phytoplankton blooms in the Nova Scotian Shelf–Gulf of Maine region: remote sensing and modeling analysis. Journal of Plankton Research, 32: 1485–1499.

Steele, J. H., Collie, J. S., Bisagni, J. J., Gifford, D. J., Fogarty, M. J., Link, J. S., Sullivan, B. K., *et al.* 2007. Balancing end-to-end budgets of the Georges Bank ecosystem. Progress in Oceanography, 74: 423–448.

Stevenson, T. J., Visser, M. E., Arnold, W., Barrett, P., Biello, S., Dawson, A., Denlinger, D. L., *et al.* 2015. Disrupted seasonal biology impacts health, food security and ecosystems. Proceedings of the Royal Society B: Biological Sciences, 282: 20151453.

Stock, C. A., John, J. G., Rykaczewski, R. R., Asch, R. G., Cheung, W. W. L., Dunne, J. P., Friedland, K. D., *et al.* 2017. Reconciling fisheries catch and ocean productivity. Proceedings of the National Academy of Sciences of the United States of America, 114: E1441–E1449.

Thomas, A. C., Pershing, A. J., Friedland, K. D., Nye, J. A., Mills, K. E., Alexander, M. A., Record, N. R., *et al.* 2017. Seasonal trends and phenology shifts in sea surface temperature on the North American northeastern continental shelf. Elementa: Science of the Anthropocene, 5: 1–17.

Townsend, D. W., Pettigrew, N. R., Thomas, M. A., Neary, M. G., McGillicuddy, D. J., and O'Donnell, J. 2015. Water masses and nutrient sources to the Gulf of Maine. Journal of Marine Research, 73: 93–122.

Townsend, D. W., Rebuck, N. D., Thomas, M. A., Karp-Boss, L., and Gettings, R. M. 2010. A changing nutrient regime in the Gulf of Maine. Continental Shelf Research, 30: 820–832.

Townsend, D. W., Thomas, A. C., Mayer, L. M., Thomas, M., and Quinlan, J. 2006. Oceanography of the Northwest Atlantic continental shelf. *In* The Sea, pp. 119–168. Ed. by Robinson A. R., and Brink K. H.. Harvard University Press, Cambridge.

Trombetta, T., Vidussi, F., Mas, S., Parin, D., Simier, M., and Mostajir, B. 2019. Water temperature drives phytoplankton blooms in coastal waters. PLoS One, 14: e0214933.

Xu, Y., Miles, T., and Schofield, O. 2020. Physical processes controlling chlorophyll-a variability on the Mid-Atlantic Bight along northeast United States. Journal of Marine Systems, 212: 103433.

Xu, Y., and Ramanathan, V. 2012. Latitudinally asymmetric response of global surface temperature: implications for regional climate change. Geophysical Research Letters, 39: L13706.

Zang, Z., Ji, R., Feng, Z., Chen, C., Li, S., and Davis, C. S. 2021. Spatially varying phytoplankton seasonality on the Northwest Atlantic Shelf: a model-based assessment of patterns, drivers, and implications. ICES Journal of Marine Science, 78: 1920–1934.

Zinkann, A-C., Wooller, M. J., O'Brien, D., and Iken, K. 2021. Does feeding type matter? Contribution of organic matter sources to benthic invertebrates on the Arctic Chukchi Sea shelf. Food Webs, 29: e00205.

Handling Editor: C. Brock Woodson